

## Effect of Surfactant Architecture on the Properties of Polystyrene–Montmorillonite Nanocomposites

Ranya Simons,<sup>†,‡</sup> Greg G. Qiao,<sup>\*,†</sup> Clem E. Powell,<sup>†</sup> and Stuart A. Bateman<sup>\*,‡</sup>

<sup>†</sup>Polymer Science Group, Department of Chemical and Biomolecular Engineering, University of Melbourne, Parkville, VIC 3010, Australia, and <sup>‡</sup>Materials Science and Engineering, CSIRO, Graham Road, Highett, VIC 3190, Australia

Received December 22, 2009. Revised Manuscript Received January 27, 2010

A series of surfactants were designed and synthesized for use as clay modification reagents to investigate the impact of their chemical structure on the nanocomposites morphology obtained following polymerization. The behavior of the surfactant-modified clays at three different stages were investigated: after ion exchange, following dispersion in styrene monomer, and once polymerization was complete. The propensity of the styrene monomer to swell the surfactant-modified clay was observed to be a useful indicator of compatibility and predictor of the resultant polystyrene nanocomposite morphology which was directly observed using small-angle X-ray scattering (SAXS) and cryogenic transmission electron microscopy (TEM). It was found that the key components of surfactant design driving exfoliated morphologies were (1) the position of the ammonium group, (2) the inclusion of a polymerizable group, (3) the solubility of the surfactant in the monomer, (4) the length of the alkyl chain, and (5) sufficient concentration of surfactant used to exchange the clay. This understanding should lead to better design of clay modifications for use in polymer nanocomposites.

### 1. Introduction

Polymer–clay nanocomposites represent an attractive alternative to conventional polymer composites considering that significant physical property improvements can be achieved at very low clay concentration.<sup>1–3</sup> Such advantages and the resultant flow on benefits in rheology and density have been captured commercially through the use of polymer–clay nanocomposites in automobile components, packaging, and construction materials.<sup>1,2</sup> Dispersion or “exfoliation” of montmorillonite (MMT) clay into its individual clay platelets within a polymer matrix is known to depend on the polarity and structure of the polymer and the interaction between the clay and the polymer.<sup>4</sup> Previous investigations have focused on either modifying the clay to become more organophilic or the polymer to become more hydrophilic in order to improve the compatibility of the clay and polymer.

Polystyrene–clay nanocomposites prepared through both *in situ* polymerization and melt processing techniques have been

investigated.<sup>5–13</sup> Several groups have probed the effect of different clay modifiers on platelet dispersion, specifically different alkyl- or arylammonium<sup>4,10,12</sup> or alkylphosphonium surfactants<sup>6,7</sup> cation exchanged with the clay. More recently, surfactants which are capable of copolymerizing with monomers like styrene have been investigated.<sup>4–6,8,11,14,15</sup> Nonpolymerizable surfactant-modified clays resulted in intercalated polystyrene–clay nanocomposite morphologies, while the polymerizable surfactants provided predominately exfoliated morphologies. The latter observations were attributed to the surfactant participating in the polymerization reaction. Taking a different tact, Lee et al.<sup>16</sup> prepared styrene nanocomposites using montmorillonite that had been intercalated with a cationic radical initiator. Exfoliated structures were formed due to the predominant intragallery polymerization over the extra-gallery polymerization using the anchored radical initiator. Zang et al.<sup>17</sup> ion-exchanged polystyrene-based quaternary ammonium ions onto montmorillonite to form polystyrene montmorillonite composites and formed mixed intercalated/exfoliated structures, without calculating the amount of polystyrene which was exchanged onto the clay.

Despite previous efforts, the intercalation mechanisms are not well understood.<sup>1</sup> Furthermore, the essential surfactant design (structural) features required to realize exfoliated platelet morphologies remains unclear, including the position of the ammonium group within the surfactant, the length of the alkyl chain, and the requirement for polymerizable groups, and have not been explicitly investigated in the same study.

In this work, a series of surfactant structures were designed and synthesized for use as clay modifiers in order to study the relationship between surfactant structure and the resultant polystyrene/clay nanocomposite morphology. The objective of

\*Corresponding authors. E-mail: Stuart.Bateman@csiro.au (S.B.); gregghq@unimelb.edu.au (G.Q.).

(1) Chen, B. *Br. Ceram. Trans.* **2004**, *103*(6), 241–249.  
(2) Usuki; Kojima; Kawasumi; Okada; Fujishima; Kurauchi; Kamigaito *J. Mater. Res.* **1993**, *8*(5), 1179–84.  
(3) Fischer, H. *Mater. Sci. Eng., C* **2003**, *23*(6–8), 763–772.  
(4) LeBaron, P. C.; Wang, Z.; Pinnavaia, T. J. *Appl. Clay Sci.* **1999**, *15*(1–2), 11–29.  
(5) Chigwada, G.; Wang, D.; Wilkie, C. A. *Polym. Degrad. Stab.* **2006**, *91*(4), 848–855.  
(6) Zhu, J.; Morgan, A. B.; Lamelas, F. J.; Wilkie, C. A. *Chem. Mater.* **2001**, *13*(10), 3774–3780.  
(7) Zhu, J.; Wilkie, C. A. *Polym. Int.* **2000**, *49*(10), 1158–1163.  
(8) Fu, X.; Qutubuddin, S. *Mater. Lett.* **2000**, *42*(1–2), 12–15.  
(9) Liu, G.; Zhang, L.; Zhao, D.; Qu, X. *J. Appl. Polym. Sci.* **2005**, *96*(4), 1146–1152.  
(10) Zhang, W. A.; Chen, D. Z.; Xu, H. Y.; Shen, X. F.; Fang, Y. E. *Eur. Polym. J.* **2003**, *39*(12), 2323–2328.  
(11) Samakande, A.; Hartmann, P. C.; Cloete, V.; Sanderson, R. D. *Polymer* **2007**, *48*(6), 1490–1499.  
(12) Vaia, R. A.; Ishii, H.; Giannelis, E. P. *Chem. Mater.* **1993**, *5*, 1694–1696.  
(13) Vaia, R. A.; Price, G.; Ruth, P. N.; Nguyen, H. T.; Lichtenhan, J. *Appl. Clay Sci.* **1999**, *15*(1–2), 67–92.

(14) Zeng, C.; Lee, L. J. *Macromolecules* **2001**, *34*(12), 4098–4103.  
(15) Fu, X.; Qutubuddin, S. *Polymer* **2001**, *42*(2), 807–813.  
(16) Uthirakumar, P.; Song, M.-K.; Nah, C.; Lee, Y.-S. *Eur. Polym. J.* **2005**, *41*(2), 211–217.  
(17) Zang, Y.; Xu, W.; Qiu, D.; Chen, D.; Chen, R.; Su, S. *Thermochim. Acta* **2008**, *474*(1–2), 1–7.

the study was to gain insights into the mechanisms behind the driving force for exfoliation to enable more rational clay modification. Montmorillonite was modified with newly designed organic surfactants through ion-exchange methodology and dispersed in polystyrene systems through *in situ* free-radical polymerization. The newly designed surfactants varied in structure in several ways in order to study the effect of (a) the position of the ammonium group (head or tail), (b) the inclusion of a polymerizable group, and (c) the length of the alkyl chain. The behaviors of these modified clays at three different stages (after ion-exchange onto montmorillonite, the modified clay dispersed in styrene monomer, and in polystyrene composites) were investigated. Small-angle X-ray scattering (SAXS) and cryogenic TEM were used to study the modified clay/monomer interactions. The structure and properties of the resulting composites have been determined using wide-angle X-ray scattering (WAXS), transmission electron microscopy (TEM), dynamical mechanical thermal analysis (DMTA), and thermal gravimetric analysis (TGA).

## 2. Experimental Section

**2.1. Materials.** Styrene (99%) was purchased from Sigma-Aldrich and purified by passing through a basic alumina (Aldrich) column. Methanol, chloroform, diethyl ether, and ethyl acetate were purchased from British Drug Houses (BDH) Ltd. and used without further purification. Tetrahydrofuran (THF) was distilled from sodium benzophenone ketyl and sodium metal under argon and stored over 4 Å molecular sieves. Dodecyltrimethylammonium chloride (98%), 4-vinylbenzyl chloride (90%), *N,N*-dimethyldodecylamine (97%), *N,N*-dimethylhexylamine, 2,6-di-*tert*-butyl-*p*-cresol (BHT), 1,5-dibromopentane (97%), 1,11-dibromoundecane (98%), ethylbenzyl chloride (70% 4-ethylbenzyl chloride, 30% 2-ethylbenzyl chloride), magnesium flakes, lithium chloride (LiCl), copper(I) chloride (CuCl<sub>2</sub>), 1,1-diphenylpicrylhydrazyl (95%), and trimethylamine hydrochloride (98%) were purchased from Sigma-Aldrich and used without further purification. The initiator 2,2-azobis(2-methylpropionitrile) (AIBN) (DuPont Australia Vazow 64) was recrystallized from ethanol and stored below 4 °C prior to use. Sodium montmorillonite (Na-MMT) was obtained from Southern Clay Products and had a cation exchange capacity (CEC) of 92 mequiv/100 g clay.

**2.2. Characterization of Nanoclays and Nanocomposites.** Fourier transform infrared (FTIR) was used to observe the chemical modification of the clay via a Bruker FTIR/NIR with a resolution of 4 cm<sup>-1</sup>. Clay was ground into KBR powder and pressed into disks prior to being placed in the FTIR for scanning. <sup>1</sup>H NMR spectra were collected in deuterated chloroform (CDCl<sub>3</sub>) using a Varian Unity Plus 400 MHz spectrometer using tetramethylsilane (TMS) and the deuterated solvent as lock and residual solvent.

Critical micelle concentration (cmc) determination was performed using the conductivity method.<sup>18</sup> Solutions with a range of concentrations were made and the conductivity measured using a TPS WP-81 conductivity probe. The point at which the gradient of the curves changed corresponded to the cmc.

Cryogenic transmission electron microscopy (cryo-TEM) was performed on a Tecnai TF30 300 kV transmission electron microscope on styrene/clay solutions that had been frozen cryogenically onto a coated copper grid by pipetting a drop of the liquid onto a grid and quickly blotting and freezing in liquid ethane to form a frozen film.

The dynamic mechanical behavior of the cured samples was measured on a Pyris Diamond dynamical mechanical analyzer (DMA) using rectangular samples in tension. The glass transition temperature (*T*<sub>g</sub>) was determined at the maximum tan δ in the dynamic mechanical thermal analysis spectrum at 1 Hz.

Small-angle X-ray scattering (SAXS) was undertaken on the SAXS/WAXS beamline at the Australian Synchrotron, Victoria, Australia, at an energy of 12 keV for *q* values between 0.05 and 0.65 Å<sup>-1</sup>. Styrene/clay solutions were contained in 1.5 mm diameter quartz capillaries. Scattering data were calibrated for background scattering and normalized to the primary beam intensity.

Wide-angle X-ray scattering (WAXS) was performed on a Phillips PW 1729, Cu Kα<sub>1</sub> source λ = 0.154 nm. For WAXS of the nanoclays 3 g of clay was pressed into a sample holder and placed in the diffractometer. For the nanocomposites themselves a 4 mm thick polymer sample was prepared via injection molding, fitted to the sample holder, and placed in the diffractometer for scanning. The 2θ angles were varied between 1.5° and 30° in order to measure the *d*<sub>001</sub> spacing of the montmorillonite.

Thermal gravimetric analysis (TGA) was performed on both the clays and the resulting nanocomposites using a Perkin-Elmer-7 TGA. 5–8 mg of sample was heated from 50 to 800 °C using a scan speed of 15°/min.

To image the composites, 70–90 nm sections of the composite samples were microtomed at room temperature using an Ultracut E microtome at a cutting speed of 0.05 mm/s. A Jeol 100S TEM was used at 100 keV to study the dispersion of clay particles in polystyrene.

**2.3. Synthesis of Surfactants.** The structures of the surfactants used in this study are shown in Figure 1. The structures of the *N,N*-dimethyl-*N*-(4-vinylbenzyl)hexan-1-aminium (6H) and *N,N*-dimethyl-*N*-(4-vinylbenzyl)dodecan-1-aminium (12H) were synthesized based on the method of Morimoto et al.,<sup>19</sup> and the structures were confirmed by <sup>1</sup>H NMR. *N,N*-Trimethyl-6-(4-vinylphenyl)hexan-1-aminium (6T) was synthesized based on the method of Wu et al.<sup>20</sup>

*N,N*-Trimethyl-12-(4-vinylphenyl)dodecan-1-aminium (12T) was a new surfactant, and the synthesis was based on the method of Wu et al.<sup>20</sup> with modifications to account for the longer alkyl chain. 4-Vinylbenzyl chloride (0.045 mol, 6.93 g) in 20 mL of dry diethyl ether was added to a stirred suspension of magnesium flakes (0.09 mol, 2.19 g) in 20 mL of dry diethyl ether at room temperature, under argon for 30 min using 0.1 g of iodine as a catalyst. The Grignard reagent was transferred via a canular over a period of 30 min to a stirred solution of 1,11-dibromoundecane (0.045 mol, 14.04 g) in dry THF (40 mL) at room temperature, with LiCl and CuCl<sub>2</sub> as catalyst (200 and 100 ppm, respectively). The mixture was stirred overnight at room temperature. The reaction mixture was then filtered, and the filtrate was concentrated in vacuum. The concentrate was diluted in ether, and 20 mL of 0.2 N HCl was added to the mixture to stop the reaction. The organic layer was subsequently extracted with saturated hydrogen carbonate solution, followed by saturated brine solution. The ether layer was dried over MgSO<sub>4</sub> and concentrated under vacuum. The concentrate was distilled under vacuum in the presence of 1,1-diphenylpicrylhydrazyl to remove unreacted dibromo compound. Trimethylamine was made by mixing trimethylamine hydrochloride (0.065 mol, 6.35 g) with 32.5 mL of 0.1 M KOH for 3 days at room temperature. The distilled product was dissolved in acetone and quaternarized with trimethylamine at room temperature for 5 days. The solvent was evaporated, and the crude product was dissolved in chloroform and filtered. The solution was then precipitated in diethyl ether, washed several times in ether and hexane, and dried under reduced pressure. 3.9 g (23%) of a white crystalline compound was obtained. The structure was confirmed by <sup>1</sup>H NMR (400 MHz, CDCl<sub>3</sub>, TMS): δ 1.25 (m, 20H, -(CH<sub>2</sub>)<sub>10</sub>-), 2.9 (s, 2H, benz-(CH<sub>2</sub>)-), 3.53 (s, 9H, -N<sup>+</sup>-(CH<sub>3</sub>)<sub>3</sub>), 3.57 (m, 2H, -CH<sub>2</sub>-N<sup>+</sup>-), 5.2 (m, 1H, -CH=CH<sub>2</sub><sup>a</sup>), 5.7

(19) Morimoto, H.; Hashidzume, A.; Morishima, Y. *Polymer* **2003**, *44*(4), 943–952.

(20) Wu, H.; Kawaguchi, S.; Ito, K. *Colloid Polym. Sci.* **2004**, *282*(12), 1365–1373.

(18) Cochin, D.; Zana, R.; Candau, F. *Polym. Int.* **1993**, *30*(4), 491–498.

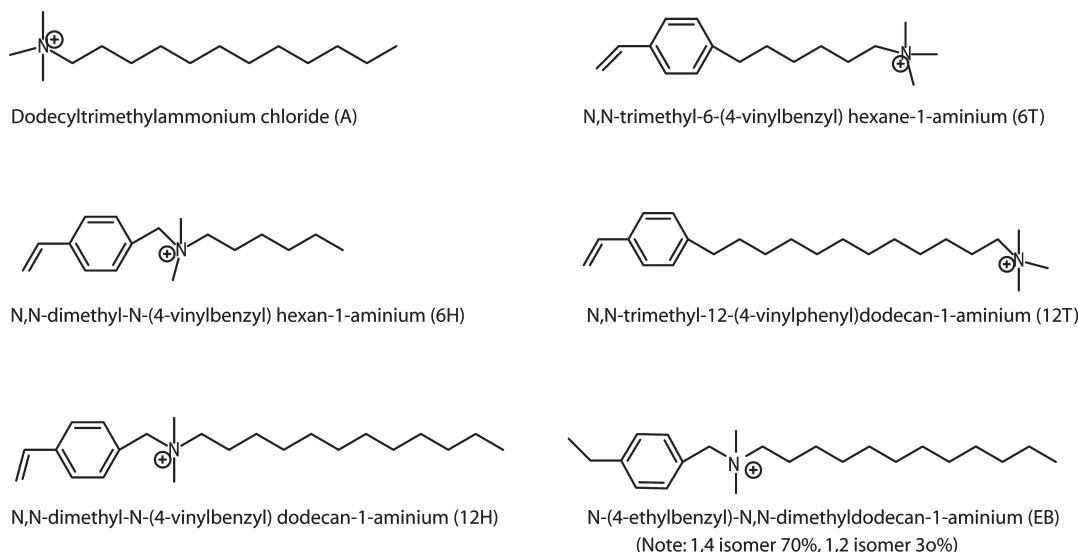


**Figure 1.** Structures of surfactants used in this study to modify montmorillonite.

(m, 1H,  $-\text{CH}=\text{CH}_2^b$ ), 6.7 (m, 1H,  $=\text{CH}-\text{benz}$ ), 7.25 (m, 4H, benzene). The compound was also verified with an accurate mass spectroscopy measurement (calculated: 330.32; actual: 330.3154).

N-(4-Ethylbenzyl)-N,N-dimethyldodecan-1-aminium (EB) was also a new surfactant and was synthesized using a modification of the synthesis for N,N-dimethyl-N-(4-vinylbenzyl)dodecan-1-aminium (12H).<sup>19</sup> In a 200 mL flask, ethylbenzyl chloride (70% 4-ethylbenzyl chloride, 30% 2-ethylbenzyl chloride) (0.0647 mol, 10 g) was mixed with N,N-dimethyldodecylamine (0.0647 mol, 13.8 g), 60 mL of ethyl acetate, and 200 ppm 2,6-di-*tert*-butyl-*p*-cresol (BHT) as inhibitor. This reaction was carried out for 72 h at 40 °C. A colorless precipitate was formed. The product was washed with diethyl ether and dried under vacuum at room temperature. The product was purified by recrystallization from acetone/diethyl ether (1/10, v/v). 18.6 g (86.3%) of a white sticky compound was obtained (containing 30% of the 2-isomer). The structure was confirmed by <sup>1</sup>H NMR (400 MHz,  $\text{CDCl}_3$ , TMS):  $\delta$  0.88 (m, 3H,  $-\text{CH}_3$ ), 1.25 (m, 18H,  $-(\text{CH}_2)_9-$ ), 1.32 (m, 3H,  $\text{CH}_3-\text{CH}_2-\text{benz}$ ), 1.79 (m, 2H,  $\text{N}^+-\text{CH}_2-\text{CH}_2-$ ), 2.7 (m, 2H,  $\text{benz}-\text{CH}_2-\text{CH}_3$ ), 3.29 (s, 6H,  $-\text{N}^+(\text{CH}_3)_2$ ), 3.5 (m, 2H,  $-\text{CH}_2-\text{N}^+-$ ), 4.97 (s, 2H,  $\text{benz}-\text{CH}-\text{N}^+$ ), 7.3, 7.6 (m, 4H, benzene).

The cmc's of the surfactants in water were determined to be A: 14.5 mmol/L, 6H: 230 mmol/L, 6T: 6.3 mmol/L, 12H: 4 mmol/L, 12T: 0.09 mmol/L, and EB: 4.25 mmol/L. These values agree well with previous calculations of similar surfactants.<sup>20</sup>

**2.4. Montmorillonite Modification.** The clay modification was based on ion-exchange methodologies.<sup>1,4,21,22</sup> Sodium montmorillonite (Na-MMT) (cation exchange capacity (CEC) = 92 mequiv/100 g) was suspended in 70 °C distilled water (20 g Na-MMT/3 L water) and stirred for 1 h. It was then allowed to cool slightly (around 40 °C). A 10% excess of the modifying ion dissolved in 250 mL of water and 1% BHT as inhibitor (dissolved in minimal ethanol) were added to the solution, and the resultant suspension was stirred without heat for a further 3 h. The resulting suspension was filtered and washed repeatedly with warm distilled water until no chloride ions were detected using 0.1 M  $\text{AgNO}_3$  solution. The resulting modified clay was preliminary dried (75 °C) for 12 h, ground to a particle size of less than 45  $\mu\text{m}$ , and further dried at 75 °C prior to processing or analysis. The resultant modified clays are termed as A-MMT, 6H-MMT, 12H-MMT, 6T-MMT, 12T-MMT, and EB-MMT modified with surfactants A, 6H, 12H, 6T, 12T, and EB, respectively.

**2.5. Synthesis of Polystyrene–Montmorillonite Composites.** The bulk polymerization method of styrene was performed based on prior work.<sup>8,15</sup> The required amount of styrene monomer was charged into a round-bottom flask with the required amount of clay. The mixture was stirred by vortex for 1 h and sonicated for 4 h to ensure proper dispersion of the clay. The mixture was degassed with argon for 20 min prior to addition of 0.5 wt % AIBN initiator. The mixture was then polymerized in an oil bath at 60 °C for 48 h to obtain polystyrene nanocomposites. The solid polystyrene was dissolved in the minimum amount of chloroform, precipitated in methanol, and dried under vacuum to afford the polystyrene nanocomposites. To form bars for mechanical and chemical testing, the nanocomposites were put through a DSM—small scale twin screw extruder with injection molder—to form bars with a width of 1 cm and length of 8 cm. The molding was performed on a 15  $\text{cm}^3$  microcompounding extruder and injection molder (DSM, The Netherlands) at a melt temperature of 185 °C, a residence time of 5 min, and a screw speed of 65 rpm. The injection molder had the injector barrel set at 195 °C, a mold temperature at 40 °C, and a pressure at 60 psi.

### 3. Results and Discussion

Quaternary ammonium ions have been widely used to modify clays for use as polymer fillers. They improve the compatibility of hydrophilic clay with organic polymers by changing the surface polarity of the clay to better suit the polarity of the polymer.<sup>23</sup> For polystyrene–clay composites, well-dispersed nanocomposites are most likely to occur when a reactive functionality is incorporated into the modifying surfactant.<sup>24</sup>

In this study, a series of surfactants were designed and then synthesized for use as clay modifiers in order to investigate the effect of the architecture of the surfactant on the resultant nanocomposites. Figure 1 shows the structures (and abbreviations) of the different organic modifications used to change the surface properties of montmorillonite. The surfactants were varied to show the effect of changing (a) the position of the ammonium group within the surfactant, (b) the presence of a polymerizable group, and (c) the length of the alkyl chain.

The 6H, 12H, 6T, and 12T surfactants contain a styrene group, which can react with styrene during the *in-situ* polymerization and

(21) Suh, D. J.; Lim, Y. T.; Park, O. *Polymer* **2000**, 41(24), 8557–8563.

(22) Xu, L.; Lee, L. J. *Polym. Eng. Sci.* **2005**, 45(4), 496–509.

(23) de Paiva, L. B.; Morales, A. R.; Valenzuela Díaz, F. R. *Appl. Clay Sci.* **2008**, 42(1–2), 8–24.

(24) Carastan, D. J.; Demarquette, N. R. *Int. Mater. Rev.* **2007**, 52(6), 345–380.



hence increase the movement of the clay platelets to increase disorder. The styrenic group is attached to the alkyl chain in either the *head* position adjacent to the ammonium group (H) or the *tail* position at the end of the alkyl chain (T). The alkyl chain length varies from either 6 or 12 units in order to investigate what effect the size of the surfactant has. Surfactant EB is a new molecule and was selected to implicitly investigate the need for a polymerizable group; it has an identical structure to surfactant 12H apart from an ethyl group instead of a vinyl group. An alkylammonium surfactant (A) with the chain length of 12 was also used as a comparison to determine the importance of including the styrene group.

While *head*-type surfactants such as 6H and 12H have been investigated in the past in styrene–montmorillonite systems,<sup>8</sup> the effect of *tail*-type surfactants such as 6T and 12T have not been investigated, and the comparison of both can provide insights into their effects. It was initially postulated that for the *tail*-type isomer the position of the styrenic functionality on the opposite end of the surfactant to the ammonium group (and hence the ion exchange site) could mean that the styrene group would be more accessible to styrene monomer during the polymerization than in the case of the *head*-type surfactants and hence lead to better dispersed systems. It is known that isomers of surfactants of this structure result in polymers with very different properties;<sup>20</sup> however, the impact of isomer on clay modification and resultant composites has not been investigated in the past.

The cmc's of the surfactants were calculated and are reported in section 2.3. The cmc's of the *tail*-type surfactants (6T and 12T) were 2 orders of magnitude smaller than the values for the *head*-type surfactants (6H and 12H), which has also been observed in the past.<sup>20</sup> This indicates that the *tail*-type surfactants form micelles more easily and at lower concentrations than the *head*-type surfactants. The *head*-type surfactants are less likely to form micelles because of the structure of the surfactants containing the hydrophilic ammonium ion between two hydrophobic regions and hence have higher cmc values. The molecules would need to twist or bend to form micelles. The EB surfactant has a similar cmc to the 12H surfactant because the structures of the surfactants are very similar. For the 12H, 12T, and EB surfactants, the ion exchange onto the clay (at 5.66 mmol/L) was performed at a concentration above the cmc. For the 6T, 6H, and A surfactants the ion exchange was performed below the cmc. Because of the large amount of agitation during the ion-exchange process, however, the surfactants are most likely not in micelles during the ion exchange.

**3.1. Modification of Montmorillonite with Organic Surfactants.** The various organo-modified clays studied in this work were characterized using WAXS, FTIR, and TGA to measure the exchange level of the organo groups to the intergallery spacing both qualitatively and quantitatively. FTIR was performed on the modified clays to confirm the attachment of the reactive surfactant onto the clay for 6H-MMT, 12H-MMT, 6T-MMT, and 12T-MMT, and the relevant portion of the spectra is shown in Figure 2. The peaks at 1514, 1487, 1470, and 1413  $\text{cm}^{-1}$  show the styrene stretches and confirm the attachment of the styrene onto the clay.<sup>25</sup> The peak at 1413  $\text{cm}^{-1}$  corresponds to the double bond stretch from the styrene group, and the observation of this stretch provides evidence that the reactive group is preserved during the ion-exchange reaction.<sup>25,26</sup> The peak at 1514  $\text{cm}^{-1}$  corresponds to the phenyl ring.<sup>27</sup> The other characteristic styrene stretches at

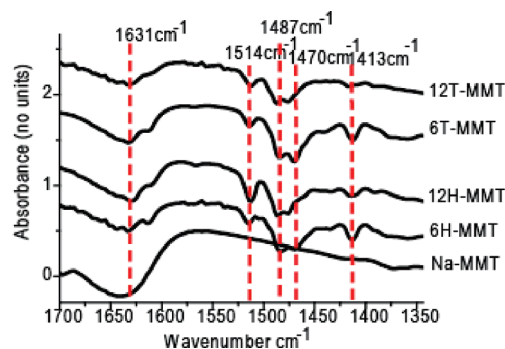


**Figure 2.** Fourier transform infrared (FTIR) spectra of Na-MMT, 6H-MMT, 12H-MMT, 6T-MMT, and 12T-MMT, confirming the presence of reactive surfactant on the clay surface.

**Table 1. Basal Spacings via WAXS and Organic Content via TGA for Modified and Unmodified Montmorillonite**

clay	basal spacing ( $d_{001}$ , Å) of modified clay (WAXS)	organic content (%) of modified clay (TGA)	% exchanged of cation exchange capacity (CEC)
Na-MMT	11.7		
A-MMT	15.7	15	71
6H-MMT	14.5	19	84
12H-MMT	18.8	25	82
6T-MMT	14.5	20	88
12T-MMT	14.3	21	69
EB-MMT	18.3	24	79

around 1631, 1000, and 890  $\text{cm}^{-1}$  are hidden by the strong peaks from the MMT.

The basal spacings of the clays were calculated from WAXS spectra for the modified and unmodified montmorillonite, and they are shown in Table 1.

All modified clays exhibited an increase in basal spacing. The A-MMT, 6H-MMT, 6T-MMT, and 12T-MMT exhibited only modest increases in the basal spacing (14–15.7 Å). The 12H-MMT has the largest increase at 18.8 Å, followed by the EB-MMT with a spacing of 18.3 Å. The orientation of alkylammonium ions within montmorillonite has been investigated in the past,<sup>28</sup> and it has been found that alkylammonium ions may lie parallel to the clay surface as a monolayer (corresponding to a  $d_{001}$  of 1.4 nm), a lateral bilayer (corresponding to a  $d_{001}$  of 1.8 nm), a pseudotrimolecular layer (corresponding to a  $d_{001}$  of 2.3 nm), or an inclined “paraffin” structure (corresponding to a  $d_{001}$  of 4.6 nm). If these reactive surfactants behave similarly to alkylammonium ions in clay, the observation of larger basal spacings for 12H-MMT and EB-MMT suggests that these surfactants were orientated in a bilayer arrangement between the clay layers. Similarly, it is most likely that the 6H-MMT, 6T-MMT, 12T-MMT, and A-MMT surfactants were arranged in a monolayer. This indicates that the presence of the bulky styrene group adjacent to the ammonium ion in the *head*-type arrangement influences the orientation of the surfactants within the clay layers, and the position of the ammonium group in combination with the higher alkyl chain length is responsible for the increase in the basal spacing for the 12H-MMT and EB-MMT. This is surprising as it is opposite to the initial expectations of the surfactant structure design that the 12T-MMT would lead to a modified clay with more accessible functional groups.

TGA analysis of the modified clays was used to determine the extent of cation exchange. Direct quantitative analysis of the organic

(25) Khalil, H.; Mahajan, D.; Rafailovich, M. *Polym. Int.* **2005**, 54(2), 423–427.

(26) Bachiller-Baeza, B.; Anderson, J. A. *J. Catal.* **2002**, 212(2), 231–239.

(27) Bellamy, L. J. *The Infra-red Spectra of Complex Molecules*; Chapman and Hall: London, 1975.

(28) Lagaly, G. *Solid State Ionics* **1986**, 22, 43–51.

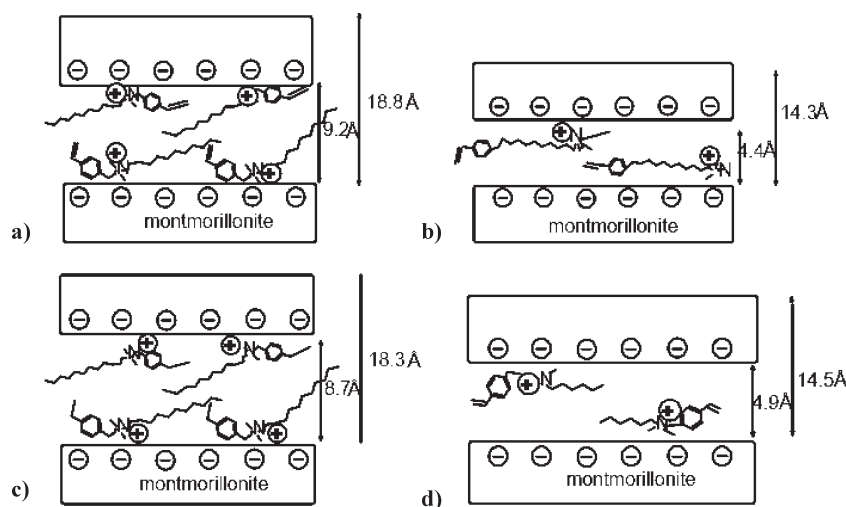


**Figure 3.** Possible orientations of the surfactants within the clay layers for (a) 12H-MMT, (b) 12T-MMT, (c) EB-MMT, and (d) 6H-MMT. The outer arrows indicate the basal spacing (which includes the thickness of one silicate layer at 9.6 Å plus the distance between silicate layers), and the inner arrows indicate the distance between galleries only.

layer was calculated by subtracting the mass loss due to physisorbed water (occurs around 170 °C) and to dehydroxylation of the mineral (occurs around 550–680 °C) from the total mass loss.<sup>29</sup>

Table 1 lists the calculated organic content of the modified clays from the TGA data as well as the organic content as a percentage of the cation exchange capacity (CEC) of montmorillonite. The surfactants used in the study were exchanged to 69–88% of the available sites, which is comparable to similar surfactants used to modify clay in the past.<sup>15,29</sup> For comparison, clays exchanged for a longer period of 24 h were also investigated, and no further increase in the exchanged amount of surfactant was observed.

It has been suggested that for molecules with unsaturated aromatic compounds such as styrene, the molecules tend to prefer the parallel orientation when intercalated between clay layers, in order to present the dipole parallel to the surface.<sup>30</sup> There has also been evidence of concentration dependence—lower concentrations favor the parallel orientation, while higher concentrations tend to favor the perpendicular structure. Combining this knowledge with observed basal spacing from WAXS, the possible orientation of the surfactants is postulated in Figure 3.

The models suggest that for 12H-MMT and EB-MMT the alkyl chain of the surfactant is freer to move in a bilayer, whereas in 12T-MMT the molecule lies flat along the clay surface due to interaction with the silicate surface at both ends of the molecule (the ammonium ion and the styrene group), forming a monolayer. This orientation of the 12T-MMT could also mean that surfactants lying flat along the clay surface are obstructing ion exchange sites and thus limit complete ion exchange of the clay as observed via TGA (Table 1) which showed that the 12T-MMT clay had the lowest amount of cation exchanged onto the clay (69%). For the 6H-MMT, the alkyl chain is not long enough to form a bilayer structure as it does with the 12H-MMT, despite the styrene group being in the head position of the molecule and so also forms a monolayer. These models of the surfactant orientations likely account for the differences in basal spacing observed. Another possible intergallery structure is that the surfactants are inclined at an angle rather than forming a mono- or bilayer. Because of the likelihood of interaction between the styrene and the silicate surface, the monolayer/bilayer structure is more likely, as postulated in Figure 3.

**3.2. Swelling of Organo-Clay in Styrene Monomer Solution.** To understand the behavior of modified montmorillonite in the styrene monomer solution, and relate this to final nanocomposite morphologies, solution SAXS and cryogenic-TEM were performed on the styrene monomer solutions containing organo-clays after vortex mixing and sonification. It has been observed that an important indicator of the chemical compatibility between organo-clay and a solvent or monomer is the swelling behavior of the clay in the solvent or monomer, with higher swelling degrees leading to better dispersion in the final composite.<sup>31,32</sup>

The observed visual swelling of the organo-clays in styrene monomer is detailed in Table 2. While the unmodified clay exhibited no swelling, A-, 6H-, 6T-, and 12T-MMT exhibited partial swelling. 12H-MMT swelled completely and caused gelling of the solution upon sonification, while EB-MMT appeared to swell completely but only partially gelled. This gel effect of MMT in styrene has been observed previously by Fu et al.<sup>15</sup> The viscosity increase and gelation by organophilic clay dispersed in organic media are most likely due to the expansion and delamination of clay layers and structure formation between the layers due to strong hydrogen bond or ionic interaction at the edge-to-edge and edge-to-face contacts.<sup>33</sup> This gelation is a good indication that the clay and styrene are chemically compatible for these organoclays.

While it has been observed that the swelling of clay in monomer or solution is a good indication of the compatibility of the clay with the monomer,<sup>31</sup> the effect of clay swelling in monomer on the basal spacing, to our knowledge, has not been investigated in the past. In this work, the styrene monomer–clay solution after vortex and sonication was measured using small-angle X-ray spectroscopy (SAXS) and the basal spacing data presented in Table 2. All clays exhibit an increase of the basal spacing upon addition of the styrene. This increase indicates that styrene is intercalating between the clay layers. The largest increases were observed for 12H-MMT and EB-MMT, corresponding to the best visual swelling and gelation and highest initial basal spacing of clay. Many of the clay–styrene solutions exhibited two  $d_{001}$

(29) Osman, M. A.; Ploetze, M.; Suter, U. W. *J. Mater. Chem.* **2003**, *13*, 2359–2366.

(30) Theng, B. K. G. *Clays Clay Miner.* **1971**, *19*, 383–390.

(31) Arioli, R.; Gonçalves, O. H.; Castellares, L. G.; da Costa, J. M.; Araújo, P. H.; Machado, R.; Bolzan, A. *Macromol. Symp.* **2006**, *245–246*(1), 337–342.

(32) Burgentzlé, D.; Duchet, J.; Gérard, J. F.; Jupin, A.; Fillon, B. *J. Colloid Interface Sci.* **2004**, *278*(1), 26–39.

(33) Granquist, W. T. M.; L, J. *J. Colloid Sci.* **1963**, *18*, 409–420.

**Table 2. Solubility of Surfactants in Styrene and Observed Swelling and Basal Spacing of 5% Modified Clay in Styrene Solution via SAXS**

clay	swelling of organo-clay in styrene (visual)	basal spacing ( $d_{001}$ , Å) of 5% clay in styrene monomer (SAXS)	solubility of surfactant (not attached to MMT) in styrene (g/mL)
Na-MMT	none	10.8	
A-MMT	partial	15.7, 35 (broad, very weak)	0
6H-MMT	partial	22.6, 14.3	0
12H-MMT	complete	16.7, 35	0.8
6T-MMT	partial	15.5	0
12T-MMT	partial	14.3	0
EB-MMT	complete	16.7, 33.8	0.8

peaks in the SAXS, which corresponds to two main populations of intercalated clay in the solutions. The small increase in basal spacing observed for the A-, 6H-, 6T-, and 12T-MMT–styrene solutions may be due to the monolayer arrangement of surfactant within the clay spacing which does not allow as much styrene to be intercalated within the layers. The solubility of the surfactants (when not attached to clay) in styrene was also tested in correlation with the swelling behavior (Table 2). The 12H and EB surfactants were the only surfactants soluble in styrene monomer, and the modified clays arising from these surfactants show the best compatibility in styrene monomer as observed visually and in the SAXS data. This suggests that during the styrene swelling phase the surfactants 12H and EB assume more of a vertical position within the clay layers because they are soluble in styrene, adopting these orientations to minimize energy and thus increasing in basal spacing.

SAXS and WAXS can only measure the clay structure that is still ordered within the styrene; any disordered clay that arises from exfoliation is not observed from these techniques, and so only partial information is gleaned from these techniques. To directly observe the clay dispersions in styrene monomer, cryogenic-TEM images of 2.5% Na-MMT–styrene, 2.5% 12H-MMT–styrene, and 2.5% 12T-MMT–styrene solutions were obtained and are shown in Figure 4.

To our best knowledge, this is the first time the clay dispersion states have been directly observed in monomer solutions by cryogenic TEM. In the Na-MMT–styrene solution (Figure 4A), there is indication of large tactoids (groupings of clay platelets associated closely together) present with occasional individual platelets and some smaller tactoids. This ordered platelet structure was also observed by SAXS. The TEM of the 12T-MMT–styrene solution does not show any evidence of large tactoids, but smaller tactoids and single platelets are common (Figure 4B). The 12H-MMT–styrene shows mostly single platelets or tactoids of only a few platelets together (Figure 4D). Figure 4C shows a region where the platelets are ordered in an overlapping pattern, which may indicate possible edge-to-face<sup>34</sup> interactions. These TEM observations correspond to the swelling observations and the solution SAXS results. Overall, the swelling observations indicate that the 12H-MMT exhibits the best dispersion of clay platelets in the styrene solution, through both visual (TEM, and visual swelling) and analytical (SAXS) techniques.

**3.3. Polystyrene–Montmorillonite Nanocomposites.** Polystyrene composites with unmodified and modified montmorillonite were formed using bulk polymerization methodology. Bulk

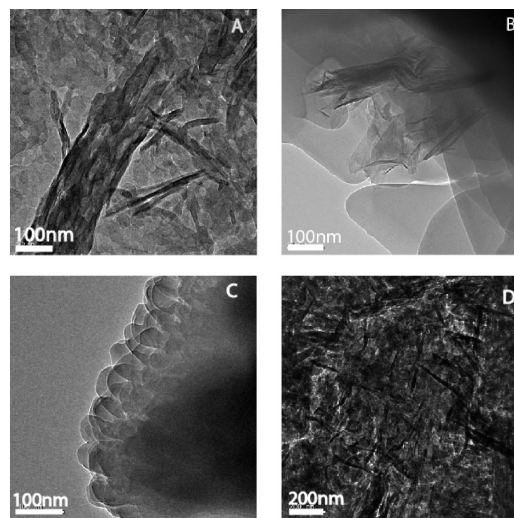


**Figure 4.** Cryogenic TEM images of (A) 2.5% Na-MMT, (B) 2.5% 12T-MMT, and (C, D) 2.5% 12H-MMT in styrene in different regions and at different magnifications.

polymerization was chosen as the method to form the nanocomposites based on work by Wang et al.,<sup>35</sup> who found that solution polymerization always formed intercalated structures whereas bulk polymerizations were more likely to form exfoliated structures. The morphology of the polystyrene–montmorillonite (referred to herein as surfactant–MMT–PS) composites was determined using TEM and WAXS, which in combination provide an indication of the dispersion of the clay within the polystyrene.<sup>36</sup> The TEM images of the 5% clay–polystyrene nanocomposites are shown in Figure 5. The basal spacing's of the 1%, 2.5%, and 5% composites as determined via WAXS are reported in Table 3, and the spectra for the 5% composites are presented in Figure 6.

TEM of 5% Na-MMT-PS (Figure 5a) indicates a poorly dispersed system with large tactoids. Minimal increase in the basal spacing was shown via WAXS (Table 3) for all concentrations, indicating that the composite was a microcomposite with poor dispersion. The TEM of the 5% A-MMT-PS nanocomposite (Figure 5b) shows a better dispersed composite of smaller clay tactoids, corresponding to a composite with clay particles still exhibiting order, and this corresponds to a very large peak as observed in the WAXS spectra (Figure 6). This structure is considered as an intercalated structure. TEM of the 5% 6H-MMT-PS, 6T-MMT-PS, and 12T-MMT-PS (Figure 5, parts c, e, and f, respectively) show platelets and tactoids of various sizes—ranging from individual platelets, smaller tactoids that are reasonably well dispersed, and tactoids up to 2  $\mu\text{m}$  in diameter, indicating intercalated structures. The WAXS spectra (Figure 6) indicate only a very slight increase in the basal spacing, which indicates that the clay is still in an ordered state (intercalated), with only a small amount of polystyrene between the clay layers. Previous work in the area has shown that polymerizable groups on the clay can sometimes lead to “pinning” of the clay layers.<sup>37–39</sup> In these cases, the one growing styrene chain will react with several styrene surfactants on the clay surface, in effect pinning the layered structure and leading to a smaller basal spacing as the regular

(36) Sinha Ray, S.; Okamoto, M. *Prog. Polym. Sci.* **2003**, 28(11), 1539–1641.

(37) Zhang, J.; Jiang, D. D.; Wilkie, C. A. *Polym. Degrad. Stab.* **2006**, 91(4), 641–648.

(38) Zhang, J.; Wilkie, C. A. *Polymer* **2006**, 47(16), 5736–5743.

(39) Zhang, J.; Jiang, D. D.; Wang, D.; Wilkie, C. A. *Polym. Degrad. Stab.* **2006**, 91(11), 2665–2674.

(34) Luckham, P. F.; Rossi, S. *Adv. Colloid Interface Sci.* **1999**, 82(1–3), 43–92.

(35) Wang, D.; Zhu, J.; Yao, Q.; Wilkie, C. A. *Chem. Mater.* **2002**, 14(9), 3837–3843.



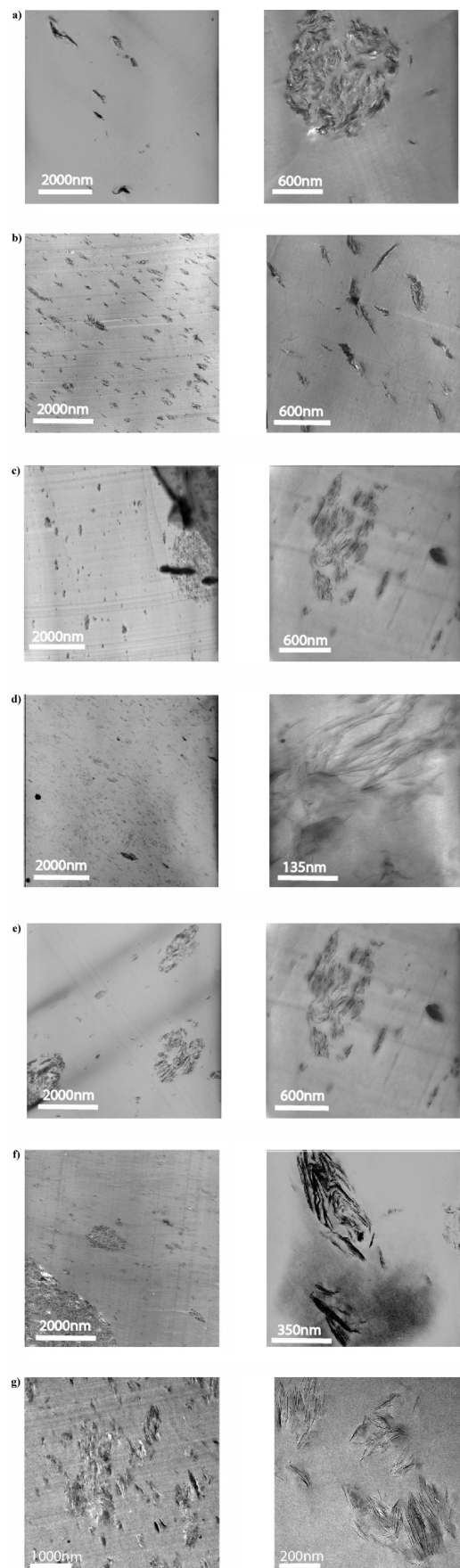


**Figure 5.** TEM images of 5% (a) Na-MMT, (b) A-MMT, (c) 6H-MMT, (d) 12H-MMT, (e) 6T-MMT, (f) 12T-MMT, and (g) EB-MMT in polystyrene composites.

**Table 3.** Basal Spacings of Clay–Polystyrene Composites at 1, 2.5, and 5 wt % As Determined via WAXS

clay	1% composite (Å)	2.5% composite (Å)	5% composite (Å)
Na <sup>+</sup> -MMT	11.8	10.5	12.3
A-MMT	13.8	13.8	13.9
6H-MMT	15.2	14.7	14.8
12H-MMT			49, 19 (broad, weak)
6T-MMT	14.7	14.4	14.8
12T-MMT	14.3	14.1	14.2
EB-MMT	18.3	17	18 (small), 33 (broad)

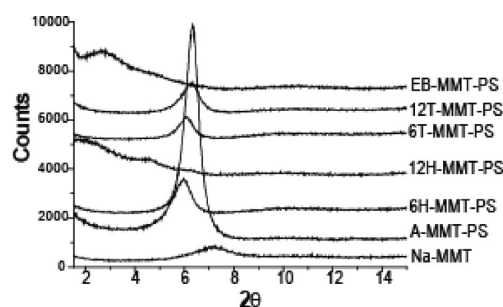


**Figure 6.** Wide-angle X-ray scattering spectra of 5% unmodified and modified montmorillonite–polystyrene composites.

structure of the clay is maintained.<sup>37–39</sup> It is possible that this is happening for these modified clays which have not exhibited vastly improved intercalation.

TEM images of the 5% 12H-MMT-PS composites show a predominantly exfoliated structure with some occasional smaller tactoids visible. From the WAXS (Table 3), at 1 and 2.5% loading, there is no evidence of a peak in the spectra, indicating no order to the clay platelets. At 5% there is a low intensity, broad peak at 48.5 Å, and a smaller peak at 19.5 Å, which corresponds to the occasional small tactoid observed in the TEM (Figure 5d). This is in agreement with earlier observations by Fu et al.,<sup>15</sup> with the same surfactant used to modify clay for polystyrene composites, and with Akelah et al.,<sup>40</sup> who used a longer chained version of this surfactant to modify montmorillonite. TEM of 5% EB-MMT-PS (Figure 5e) indicates better dispersed clay layers than in the Na-MMT-PS, A-MMT-PS, 6H-MMT, 6T-MMT, and 12T-MMT-PS systems, with some individual clay platelets visible; however, there are still small tactoids evident (corresponding to the small peak in the WAXS trace in Figure 6). It is not as well dispersed as the 12H-MMT-PS composites as observed via TEM, even at lower clay loadings, which is also confirmed by the presence of a peak at 1 and 2.5 wt % in the WAXS.

The TEM and WAXS observations indicate that the 12H-MMT-PS composites are the best dispersed systems. This can be attributed to the presence of the double bond, as the corresponding surfactant EB does not lead to as well-dispersed systems despite being identical in structure apart from the double bond. The position of the ammonium ion in the 12H-MMT in the head position is also vital, as the 12T-MMT (which varies from 12H-MMT only in the position of the ammonium group) does not lead to exfoliated structures. The length of the alkyl chain also played an important role, as the 6H-MMT-PS did not lead to well-dispersed systems. These observations are expected to apply for similarly designed surfactants that contain a reactive

(40) Akelah, A.; Rehab, A.; Agag, T.; Betiha, M. *J. Appl. Polym. Sci.* **2007**, *103*(6), 3739–3750.

group, such as for methacrylate- or acrylate-based alkylammonium ions.

Physical properties of the surfactants in water were investigated including the cmc (section 2.3). The ability of the surfactants to form micelles was not related to the final morphology of the polymer–clay nanocomposites; the 12T surfactant had the lowest cmc but only led to intercalated nanocomposites, whereas the 12H surfactant had a higher cmc but led to well-exfoliated structures. The chemical properties and structure of the surfactants have been observed to be the most important aspects of the surfactant for designing structures that can lead to well-dispersed composites.

As observed earlier, the solubility of the surfactants in styrene (Table 2) showed that only the 12H and EB surfactants were soluble in styrene. These surfactants led to the highest dispersed clay not only in styrene monomer but also in the final polystyrene composite; however, only the 12H-MMT led to completely exfoliated nanocomposites. This work demonstrates that the solubility of the surfactants in the monomer is a necessary condition for achieving exfoliation of the clay in the polymer; however, it is not a sufficient condition. Solubility testing may be an easy and quick way to screen potential surfactants for use in clay modification.

These insights into clay modifications may provide insight for other cationic clays exchanged with organic surfactants and for other free radical polymerized systems.

The work presented so far investigated clay that had been synthesized with 100% of the CEC (cation exchange capacity) with respect to surfactant loading. To study the effect of surfactant exchange level, the 6H, 12H, 6T, and 12T surfactants were also exchanged onto montmorillonite at 50% the CEC of the clay, and the resultant basal spacings are shown in Table 4. The basal spacings of these clays as determined by WAXS were less than the clays modified by 100% the CEC amount (Table 1) in all cases and were of similar value to each other. These results clearly show that the surfactants did not expand the intergallery space to the same level as in the case when there was sufficient surfactant for maximum ion exchange. For the 12H-MMT, at 50% ion exchange the surfactant is most likely forming a monolayer arrangement (with a basal spacing of 14.7 Å) in the clay spacing rather than the bilayer arrangement as hypothesized in Figure 3 for the 100% CEC exchanged clays. The corresponding 5% composites of the 50% CEC clays also exhibited lower basal spacings, including the 12H-MMT composites, which in this case did not lead to exfoliated structures (although it did when exchanged to 100% onto the clay). This demonstrated that the clay needs to be modified with 100% surfactant in order to sufficiently improve the compatibility and increase the basal spacing sufficiently for styrene to enter the spacing and polymerize within the clay layers to form exfoliated structures. These results contrast the report by Suh et al.,<sup>41</sup> who used stearylamine as a clay modifier, in which case 50% exchanged clays led to exfoliated nanocomposites, whereas 100% exchanged clays did not. They hypothesized at 50% surfactant loading there was more room within the clay layers for the polymer to intercalate. The differences in results between the reported work and the current work may be due to the different organic modifications used, where the presence of the styrene group in the surfactant in the current work is the driving force for styrene monomer to intercalate within the clay layers. Clays exchanged to 150% of the CEC were also synthesized and used as fillers in polystyrene nanocomposites (not shown). However, these composites showed similar behaviors to those at 100% CEC. This indicates excess surfactant was washed

**Table 4. Basal Spacings of Clays Modified at 50% Cation Exchange Capacity (CEC) and Corresponding Composites As Determined via WAXS**

clay	basal spacing of clay (Å)	basal spacing of polystyrene composites (5% clay loading) (Å)
6H-MMT 50% CEC	14.3	14.4
12H-MMT 50% CEC	14.7	14.7
6T-MMT 50% CEC	14.5	14.5
12T-MMT 50% CEC	14.0	14.3

away after ion exchange was complete, leaving the equivalent surfactant concentration on the clay to the 100% CEC clays.

**3.4. Physical Properties of Polystyrene–Montmorillonite Nanocomposites.** The physical properties of the polystyrene–montmorillonite composites were investigated to determine what effect the morphology of the composites had on the properties and are reported in Table 5 for nanocomposites containing 5% modified and unmodified MMT. The thermal mechanical behavior of the polystyrene composites was measured from  $-100$  to  $140$  °C on a DMTA, and the resulting storage modulus and  $T_g$  were calculated. The storage modulus  $E'$  at  $25$  °C increased for all modified clay composites by up to 119% for the 5% 12H-MMT-PS and 58% for the 5% EB-MMT-PS, whereas the unmodified clay (Na-MMT) composite decreased by 35% over unreinforced polystyrene. This is further proof that the modified clays have improved the interaction of the clay with the polystyrene, allowing the reinforcement of the clay platelets to improve the physical properties, particularly for the best dispersed systems of 5% 12H-MMT-PS and 5% EB-MMT-PS. This enhancement in storage modulus is due to the high aspect ratio of the dispersed clay, which improves the interaction between the clay layers and polymer chains, resulting in a decrease in the polymer chains mobility near the polymer–clay interface. Modulus values above the  $T_g$  ( $> 110$  °C) in the rubbery region did not exhibit a plateau value as is commonly observed as the composites melted in the sample holders, making it difficult to measure modulus values in this region.

One phase transition was observed via DMTA, corresponding to a glass transition ( $T_g$ ) of around  $110$  °C. Addition of Na-MMT decreased the  $T_g$  by 2 deg compared to unfilled polystyrene, which had a  $T_g$  of  $111$  °C. The 5% A-MMT-PS, 5% 6H-MMT-PS, 5% 6T-MMT-PS, and 5% 12T-MMT-PS had an increased  $T_g$  by 2–4 °C. The best dispersed systems of 5% 12H-MMT-PS and 5% EB-MMT-PS actually showed a slight decrease in the  $T_g$ , although these differences in  $T_g$  are not highly significant with respect to the error associated with the technique. Decreases in  $T_g$  have been observed previously for well-dispersed systems and have been attributed to the high viscosity of the styrene-modified montmorillonite solutions which affects the dispersion of initiator molecules in the bulk free radical polymerization.<sup>8</sup>

The addition of clay increases the peak differential temperature observed using TGA for the major thermal decomposition phase in the polystyrene by up to  $23$  °C. There is little difference between the unmodified Na-MMT composite and the modified clay composites which indicates that the ion exchange of a reactive styrenic functionality onto the clay does not make the resultant nanocomposite more susceptible to thermal degradation. The improvement in the thermal stability of the clay nanocomposites has been attributed to the restriction of polymer chains within and close to the silicate layers, leading to greater resistance to thermal degradation and has been noted for different clay–polymer systems.<sup>42,43</sup>

(41) Suh, D. J.; Park, O. O. *J. Appl. Polym. Sci.* **2002**, 83(10), 2143–2147.

(42) Blumstein, A. J. *Polym. Sci., Part A* **1965**, 3, 2665.

(43) Dean, K. M.; Bateman, S. A.; Simons, R. *Polymer* **2007**, 48(8), 2231–2240.



**Table 5. Thermal and Mechanical Properties of Polystyrene–Montmorillonite Composites**

sample	storage modulus $E'$ at 25 °C (Pa) <sup>a</sup>	glass transition $T_g$ (°C) <sup>b</sup>	peak degradation temperature (°C) <sup>c</sup>	char (%) <sup>d</sup> expt (calcd)
polystyrene	$1.67 \times 10^9$	111	427	0.8
5% Na-MMT-PS	$1.1 \times 10^9$	109	446	5.2 (5.15)
5% A-MMT-PS	$2.33 \times 10^9$	112	441	5.2 (4.95)
5% 6H-MMT-PS	$2.04 \times 10^9$	114	447	4.9 (4.95)
5% 12H-MMT-PS	$3.65 \times 10^9$	110	439	6.1 (4.35)
5% 6T-MMT-PS	$2.14 \times 10^9$	114	450	5.2 (4.95)
5% 12T-MMT-PS	$2.15 \times 10^9$	114	450	5.0 (4.75)
5% EB-MMT-PS	$2.65 \times 10^9$	110	442	5.3 (4.55)

<sup>a</sup> Storage modulus  $E'$  (Pa) of polystyrene and 5 wt % montmorillonite based composites from dynamic mechanical thermal analysis (DMTA). <sup>b</sup> Glass transition temperature  $T_g$  (°C) of polystyrene and 5 wt % montmorillonite based composites from dynamic mechanical thermal analysis (DMTA). <sup>c</sup> Peak differential temperature (°C). <sup>d</sup> Char % (experimental and calculated) obtained from thermal gravimetric analysis (TGA).

The peak differential temperature of the 12H-MMT-PS is lower than for the intercalated and microstructured composites but higher than pristine polystyrene. The lower thermal stability of exfoliated nanocomposites over intercalated was observed previously<sup>11</sup> and attributed to the ion-exchanged modifying surfactant having poorer thermal properties which decreases the overall stability of exfoliated samples.

The char of the clay composites is also presented in Table 5 and is calculated as the remaining mass at 700 °C as a percentage of the starting mass. The calculated char in parentheses was based on the known organic content of the modified clay as determined by TGA (section 3.1) plus the char remaining from pristine polystyrene as determined by TGA. It can be seen that the 12H-MMT-PS has the highest char and is of a higher value than the calculated char. This is an indication that the 12H-MMT-PS has improved fire-retardancy properties, as the buildup of this high-performance carbonaceous char improves retardancy due to its thermal insulating and low permeability to further degradation.<sup>44,45</sup> This increase in char has been attributed to the barrier effect,<sup>46,47</sup> which assumes the formation of a carbonaceous silicate char that builds up on the surface of the polymer melt and acts as a mass and heat transfer barrier.

#### 4. Conclusion

A series of polystyrene montmorillonite composites have been developed with differently modified clays in order to probe the effect of the structure of the organic modification on

the final nanocomposite morphology. For *in situ* free radical polymerized polystyrene–montmorillonite composites, it was determined that the important aspects of surfactant design to achieve well-dispersed and -exfoliated nanocomposites include the following:

1. The position of the ammonium ion in the surfactant. Locating the ammonium group in the *head* position (adjacent to the styrene group) led to exfoliated structures whereas locating the ammonium ion in the *tail* (at the end of the alkyl chain) only led to intercalated structures.
2. The presence of a polymerizable group which can react with the styrene monomer during polymerization.
3. The solubility of the surfactant in the styrene monomer. Soluble surfactants in styrene led to the best dispersed systems, whereas partially soluble or insoluble surfactants only led to intercalated morphologies.
4. The concentration of the surfactant exchanged on the clay. Exchanging surfactant to 100% of the clays cation exchange capacity (CEC) is necessary to lead to well-dispersed systems.
5. The length of the alkyl chain; for the *head*-modified clays, homologues of alkyl chain 6 did not lead to well-dispersed samples whereas an alkyl chain of 12 did.

The behavior of the modified clays in styrene monomer is also an important indicator of the ability of the organic modification to lead to well-dispersed composites. The physical properties were improved for the modified clay/polystyrene systems, particularly for the best dispersed clay composites. This understanding of the key criteria for surfactant design for use as clay modification agents can lead to better designed nanocomposite systems for free radical polymerized systems.

**Acknowledgment.** The authors thank Ken Goldie at the Bio21 Institute, Victoria, Australia for the cryogenic TEM images. The authors also thank Nigel Kirby and the SAXS/WAXS beamline at the Australian Synchrotron, Victoria, Australia.

(44) Gilman, J. W.; Jackson, C. L.; Morgan, A. B.; Harris, R.; Manias, E.; Giannelis, E. P.; Wuthenow, M.; Hilton, D.; Phillips, S. H. *Chem. Mater.* **2000**, *12*(7), 1866–1873.

(45) Wang, S.; Hu, Y.; Song, L.; Wang, Z.; Chen, Z.; Fan, W. *Polym. Degrad. Stab.* **2002**, *77*(3), 423–426.

(46) Gilman, J. W. *Appl. Clay Sci.* **1999**, *15*(1–2), 31–49.

(47) Bourbigot, S.; VanderHart, D. L.; Gilman, J. W.; Awad, W. H.; Davis, R. D.; Morgan, A. B.; Wilkie, C. A. *J. Polym. Sci., Part B: Polym. Phys.* **2003**, *41*(24), 3188–3213.